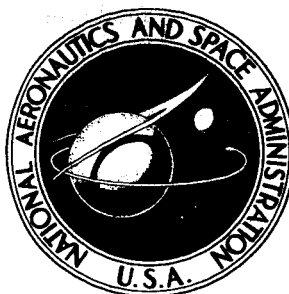


NASA CONTRACTOR REPORT



NASA CR-671

NASA CR-671

FACILITY FORM 102

N67-16011	
(ACQUISITION NUMBER)	(TITLE)
42	1
(PAGE)	(ISSUE)
CR-671	05
(NASA CR OR SPK OR TR NUMBER)	(CATEGORY)

MODEL OF HUMAN OPERATOR RESPONSE TO STEP TRANSITIONS IN CONTROLLED ELEMENT DYNAMICS

by D. H. Weir and A. V. Phatak

Prepared by
SYSTEMS TECHNOLOGY, INC.
Hawthorne, Calif.
for Ames Research Center

PRICE \$

PRICE(S) \$ 2.00

Hard Copy (HC)

microfiche (MF) 65

NATIONAL AERONAUTICS AND SPACE ADMINISTRATION • WASHINGTON, D. C. • JANUARY 1967

MODEL OF HUMAN OPERATOR RESPONSE TO STEP TRANSITIONS IN
CONTROLLED ELEMENT DYNAMICS

By D. H. Weir and A. V. Phatak

Distribution of this report is provided in the interest of information exchange. Responsibility for the contents resides in the author or organization that prepared it.

Prepared under Contract No. NAS 2-1868-4 by
SYSTEMS TECHNOLOGY, INC.
Hawthorne, Calif.

for Ames Research Center

NATIONAL AERONAUTICS AND SPACE ADMINISTRATION

For sale by the Clearinghouse for Federal Scientific and Technical Information
Springfield, Virginia 22151 - Price \$2.00

FOREWORD

This report documents a study directed toward modeling human operator response to sudden changes in the effective vehicle dynamics. The research was accomplished under Contract NAS2-1868-4 between Systems Technology, Inc., Hawthorne, California, and the Ames Research Center of the National Aeronautics and Space Administration. The NASA project monitors were M. K. Sadoff and W. E. Larsen. The STI technical director was D. T. McRuer, and the project engineer was D. H. Weir.

The bulk of the experimental data presented in this report was obtained by J. I. Elkind and his associates at Bolt, Beranek, and Newman, Inc., Cambridge, Massachusetts, and it is with their very kind permission that it has been used as the basis for the modeling activities reported herein.

The authors gratefully acknowledge the fine work of the STI Publications Department in the preparation of this report.

ABSTRACT

A model is derived for describing and predicting human operator dynamic response during sudden changes in the vehicle or controlled element dynamics. Data upon which the model is based are presented also. The model features distinct modes of behavior which are selected successively during the transition between the initial and final stationary tracking situations. The first transition mode is a retention phase which is modeled by the pretransition operator describing function in closed-loop control of the new controlled element dynamics. The next phase is characterized by nonlinear time optimal control. Finally, the operator switches to the quasi-linear describing function appropriate to closed-loop control of the new dynamics under stationary conditions.

CONTENTS

	<u>Page</u>
I. INTRODUCTION. 	1
Background. 	1
Transition Task. 	2
Report Organization.. 	3
II. TRANSITION DATA	4
Experimental Conditions	4
Data for Simplified Controlled Elements.. 	6
Data for Unstable Controlled Elements	9
Transition Duration.. 	12
III. OPERATOR RESPONSE MODEL	14
Temporal Phases of a Transition Model	14
The Resultant Transition Model. 	24
Limitations of the Transition Model. 	28
IV. CONCLUSIONS AND RECOMMENDATIONS.. 	30
Conclusions 	30
Recommendations. 	31
REFERENCES	32

FIGURES

	<u>Page</u>
1. Experimental configuration (ref. 7)	4
2. Forcing function spectrum	5
3. Transition from +8 to +2 (ref. 5).	7
4. Transition from +8 to +4/s (ref. 5)	7
5. Transition from -4/s ² to +8/s ² (ref. 5)	7
6. Transition from +2 to -8/s ² (ref. 5)	8
7. Transition from +8/s ² to -16/s ² (ref. 5)	8
8. Transition from 4/s to -8/s(s - 0.2) (ref. 8)	10
9. Transition from 4/s to +8/s(s - 0.4) (ref. 8)	10
10. Transition from 4/s to -8/s(s - 0.8) (ref. 8)	10
11. Transition from 4/s to +8/s(s - 1.0) (ref. 8)	11
12. Transition from 4/s to +8/s(s - 1.3) (ref. 8)	11
13. Phase plane trajectory for time-optimal control of K_{c2}/s^2 ..	16
14. Phase plane trajectory for time-optimal control of $K_{c2}/s(s - \alpha)$	18
15. Time-optimal control for unstable controlled element..	18
16. Ideal response for $K_{c1}/s \rightarrow K_{c2}/s(s - \alpha)$ transition..	19
17. Effect of pulseline control.. .. .	20
18. Time-optimal control for first-order system.	24
19. Phase plane trajectories for first-order system.. .. .	26
20. Time-optimal control for second-order system	27
21. Phase plane trajectories for simple second-order system ..	27

TABLES

	<u>Page</u>
I. Simplified Controlled Element Transition Data	6
II. Data Description.. .. .	21
III. Effect of Stick Reversal on Error Signal	23
IV. Mode-Switching Transition Model Summary	25

SYMBOLS

c	Operator output or stick deflection
e	System error
\dot{e}	System error rate
\ddot{e}	System error acceleration
e_0	Maximum error during transition response
i	System forcing function or input
K	Controlled element gain
K_{c1}	Pretransition controlled element gain
K_{c2}	Posttransition controlled element gain
m	System output
m_1	Output of pretransition controlled element
m_2	Output of posttransition controlled element
M	Operator output (bang) amplitude
s	Laplace transform variable
t	Time
t_0	Time of controlled element transition
t_1	Time of first control reversal
t_2	Time of second control reversal
t_3	Time of mode-switch to posttransition steady state
Y_c	Controlled element dynamics
Y_{c1}	Pretransition controlled element dynamics
Y_{c2}	Posttransition controlled element dynamics
Y_p	Quasi-linear describing function for operator dynamics
Y_{p1}	Pretransition describing function for operator dynamics

Y_{p2} Posttransition describing function for operator dynamics

α' Inverse time constant

Φ_{ii} Forcing function power spectrum

ω Angular frequency

I. INTRODUCTION

Background

The study of human operator response in the presence of rapidly changing controlled element dynamics has important implications for the manual control of aerospace vehicles. Results can be applied to vehicular control following the failure of part of the flight control system, a stability augments, or a change in the configuration such as that caused by a large shift in the center of gravity. These changes in controlled element dynamics need not be confined to emergencies, but may be a matter of routine. The manual control of boost, for example, can involve nearly steplike changes in the controlled element when staging coincides with a change in the control effectiveness due to the employment of a new set of thrusters.

There are two general types of controlled element transition. One is relatively slow, with the dynamics changing gradually over a period of a few seconds or longer. The second involves a sudden or steplike change, and this is the type of primary interest.

Sheridan (refs. 1 and 2) studied gradual changes in the controlled element from pure gain, K , to pure integration, K/s , and vice versa in both compensatory and pursuit tracking. The changes in controlled element were completed in about 6 sec, and operator adaptation as measured by the mean square error was completed in about 15 sec.

A pioneering study by Sadoff (ref. 3) compared the response of skilled pilots to steplike changes in the controlled element in both fixed-base and moving-cab simulators. A longitudinal pitch attitude tracking task was used, and the transition simulated failures of systems which augmented either static stability or pitch damping. The cab motion had a significant adverse effect in most cases on the pilot's ability to adapt to the damper failures, as evidenced by larger mean square errors during transition and longer transition times. In another experiment, the adverse effect of motion cues was reduced significantly by utilizing a side-stick manipulator with arm restraint. These results (ref. 3) represent the only extant data

for the highly realistic conditions of moving-cab simulator, aircraft-type control stick, and skilled test pilot subjects.

Extensive experimental research on operator response to step controlled element transitions has been accomplished by Elkind and associates (refs. 4-8). These studies have all involved single-axis compensatory tracking tasks in the presence of low frequency random-appearing forcing functions. A side-stick type of manipulator was used, and the facility was fixed-base. They have derived some analytical models of operator transition response, and to date these largely emphasize the detection of transition occurrence and identification of the new controlled element dynamics (e.g., refs. 9 and 10).

The study reported herein is intended to complement the previous work. It is a model building effort, with the objective of deriving an analytical model useful in predicting operator transition response. Extensive use is made of experimental data from other sources. Areas that have been treated in depth elsewhere, such as detection criteria, and the effects of learning, alerting, and uncertainty about the new dynamics are given only slight consideration.

Transition Task

The operator is assumed to be performing a single-axis compensatory tracking task in the presence of a low frequency random-appearing forcing function. Controlled element dynamics such as the forms K , K/s , or K/s^2 are used, and at the time of transition a step change is made from one form to another. The change can involve a difference in any or all of order, gain magnitude, or polarity. The operator is not alerted to the time of transition nor to what the new controlled element will be.

Transitions which yield an unstable closed-loop system when pretransition operator adaptation is retained are of particular interest, because they require immediate corrective action to retain control. This will occur for any of the following controlled element changes:

1. Sufficiently large gain increase
2. Polarity reversal

3. Increase in effective controlled element order
(for sufficiently large gain)

These are all considered in this study.

Report Organization

The second section of the report presents operator transition response data, together with a more detailed description of the experimental procedure. The data are given as time histories of forcing function, error, and operator output because the inherent nonstationarity of the process makes conventional statistical techniques inappropriate.

The third section examines and interprets the data, with the objective of modeling the operator's transition response. A "mode-switching" model is ultimately derived by induction. This model features successive phases of operator behavior, including:

1. Pretransition steady state
2. Retention of pretransition operator adaptation
3. Optimal control
4. Adjustment of posttransition steady state

The operator's entire transition response is defined for modeling purposes in terms of either duration, solution to an optimal control problem, or the quasi-linear describing function for compensatory tracking under stationary conditions. This section concludes by summarizing the limitations of the existing model.

The final section of the report presents conclusions about the derived model and transition response in general. Recommendations for additional experimental work to alleviate current deficiencies are given also.

II. TRANSITION DATA

The operator is assumed to be performing a single-axis compensatory tracking task in the presence of a low frequency random-appearing forcing function. At transition the controlled element changes instantaneously from one form to another. The problem is to determine the operator response from the time of transition until the system error returns to and remains within an acceptable threshold level following operator adaptation to the new dynamics.

Transition data resulting from a fairly complete series of experiments have been published in references 4, 5, and 8. With the kind permission of the staff of Bolt, Beranek, and Newman, Inc., these data have been used as the basis for the modeling efforts reported herein. The remainder of this section presents and describes transition response data obtained and previously published by BBN.

Experimental Conditions

The experimental configuration used is shown in figure 1. The switch is shown in the pretransition configuration with the operator, Y_p , controlling Y_{c1} in response to the displayed system error, e . The task was

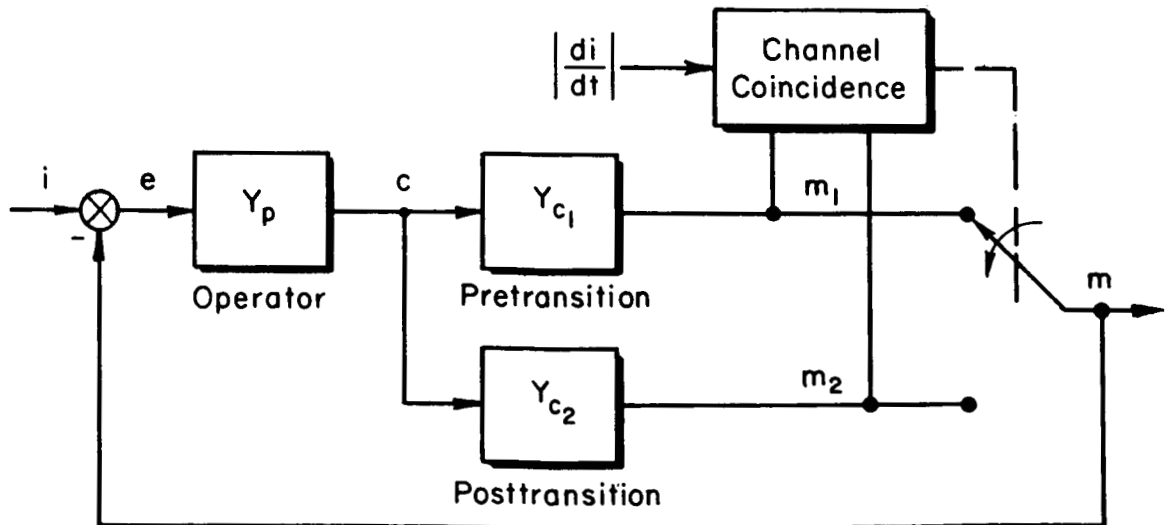


Figure 1. Experimental configuration (ref. 7)

to minimize the error. At the time of transition the switch instantaneously disconnected Y_{C1} and placed Y_{C2} in the closed loop. The channel coincidence device prevented this from occurring until the outputs m_1 and m_2 were approximately equal, and the magnitude of the input rate, $|di/dt|$, was sufficiently large. This prevented any discontinuities from occurring in the displayed error which might have alerted the operator, and the finite rate limitation insured that the system was not quiescent.

The forcing function, i , was a low frequency random-appearing signal having a rectangular spectrum with a 1.5 rad/sec cutoff frequency, as shown in figure 2. It was obtained by summing a number of equal amplitude sinusoids with noncommensurate frequencies, and hence was Gaussian to a good approximation. Because of its low bandwidth, the forcing function looked approximately like

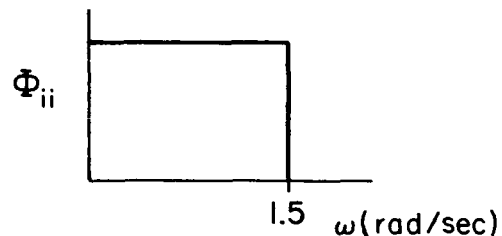


Figure 2. Forcing function spectrum

a ramp for a second or so after the transition, and like one-half of one period of a sinusoid over a 3 sec interval. These useful properties simplify the subsequent analysis of the transition response data.

The manipulator was a light control stick which protruded through a circular hole in the right arm rest of a student's chair on which the subject was seated. It had a light spring restraint, it could be moved left or right through approximately 45 deg, and it required about one pound for maximum deflection.

The operator was generally not alerted to the occurrence of the transition by any stimulus other than system error. A number of different transitions were presented in a random sequence, so the operator was uncertain about the nature of the next controlled element, and about the difference in order, gain, and polarity between successive controlled elements.

Data for Simplified Controlled Elements

In the first series of experiments considered, the pretransition and posttransition controlled elements took any of the forms K , K/s , or K/s^2 . The transition occurred at time t_0 and involved a change in any or all of order, polarity, and magnitude. Although simplified controlled elements were used, these can be good approximations, in the region of crossover, to any of a much larger class of controlled element dynamics.

The most useful data forms for analysis are time histories of stick motion, system output, and system error, because of the nonstationarity of the process. Data for the five transitions of Table I are presented in figures 3 through 7 taken from reference 5. The records are individual runs, not ensemble averages. The run-to-run variability can be estimated by comparing figures 5 and 7. Figures 4 and 6 present data for a relatively unskilled operator, and the poorer control technique is evident in the error traces. These data are exploratory, of course, and provide only a preliminary estimate of operator response technique.

Some general features of the data traces are worth discussion. The top plot in each of the five figures actually presents two traces, system forcing function and system response or output. In all cases the smoother

TABLE I
SIMPLIFIED CONTROLLED ELEMENT TRANSITION DATA
(From ref. 5)

Figure	Transition	Operator skill level
3	$+8 \rightarrow +2$	Well trained
4	$+8 \rightarrow +4/s$	Probably not well trained
5	$-4/s^2 \rightarrow +8/s^2$	Well trained
6	$+2 \rightarrow -8/s^2$	Relatively untrained
7	$+8/s^2 \rightarrow -16/s^2$	Probably well trained

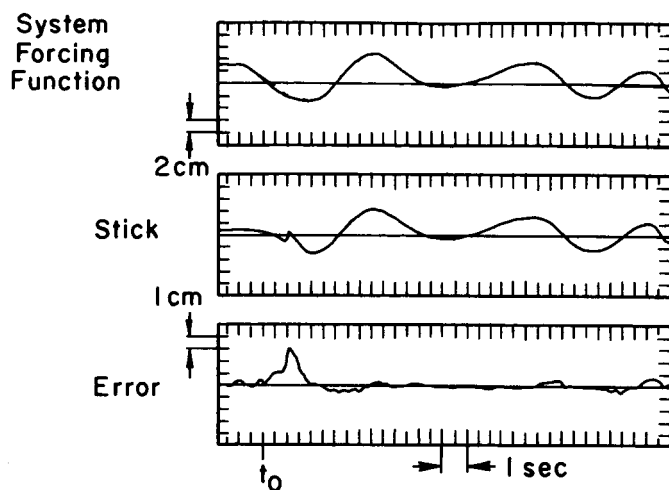


Figure 3. Transition from +8 to +2 (ref. 5)

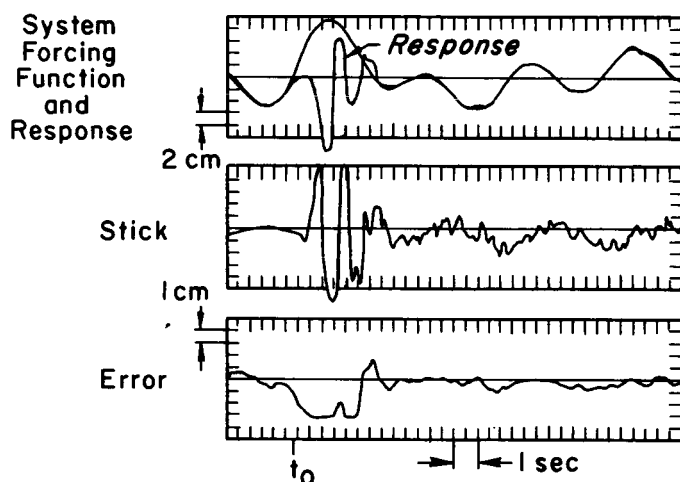


Figure 4. Transition from +8 to +4/s (ref. 5)

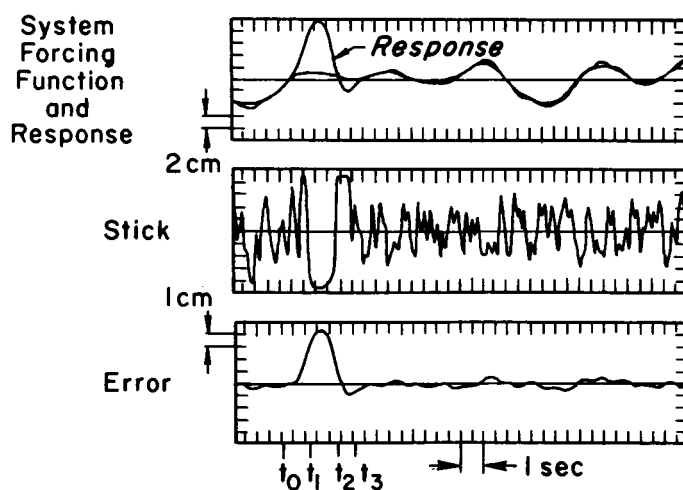


Figure 5. Transition from $-4/s^2$ to $+8/s^2$ (ref. 5)

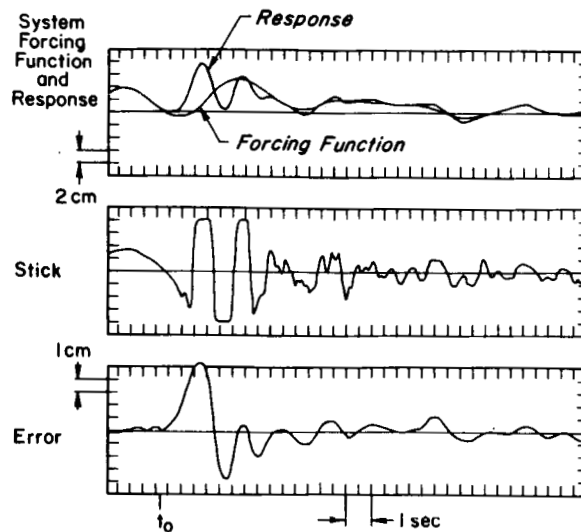


Figure 6. Transition from $+2$ to $-8/s^2$ (ref. 5)

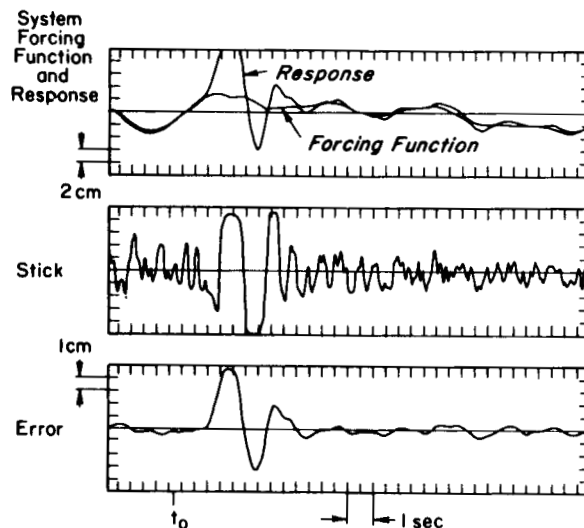


Figure 7. Transition from $+8/s^2$ to $-16/s^2$ (ref. 5)

(lower frequency content) trace is the forcing function. The stick deflection traces for the higher order controlled elements (all but fig. 3) exhibit large amplitude motions with "limiting." The fact that the large peaks are perfectly "squared off" indicates that the limiting did not happen within the operator, but occurred downstream, probably in the manipulator. Manipulator limiting is reasonable, because the side-arm stick had a travel of only ± 45 deg and required only one pound for full deflection. Thus, it would be very easy for the operator to attain a limiting deflection. Note that the displayed error did not limit.

Data for Unstable Controlled Elements

Another set of experimental results reported in reference 8 shows operator response to a step change in controlled element at time t_0 of the form

$$\frac{K_{c1}}{s} \rightarrow \frac{K_{c2}}{s(s - \alpha)}$$

The posttransition controlled element is unstable and involves an integration plus a divergent inverse time constant, $-\alpha$. Its gain may be of either sign. The data were taken under the same experimental conditions as those for the data of figures 3 through 7. The system forcing function was the low frequency random-appearing signal with a 1.5 rad/sec cutoff frequency of figure 2.

Data for eight transition runs with various values of the inverse time constant, $-\alpha$, were considered. These represent about one half of the total attempted transitions of this type. In the balance of the runs, the operator could not retain control and the experiment was aborted. Five of the eight successful runs have been selected to illustrate the results. These show representative behavior and cover a range of values for the inverse time constant. The five runs are presented in figures 8 through 12 in the order of increasing difficulty. The transition time, t_0 , is shown approximately in the figures. The times t_1 , t_2 , and t_3 shown in the figures relate to the modeling analysis of Section III.

In about one half of the runs with this transition the operator lost control, probably due to some combination of the following factors:

- Display limiting
- α too large
- Forcing function

Display limiting makes it impossible to know the state of e and \dot{e} . This, in turn, can delay the operator's switching time and result in a large overshoot and further limiting. When the inverse time constant is too large, e and \dot{e} build up rapidly and the display limits before the operator can effect control. The forcing function modifies e and \dot{e} and may cause incorrect operator response.

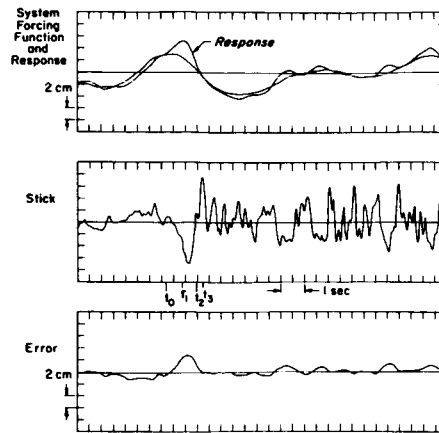


Figure 8. Transition from $4/s$ to $-8/s(s - 0.2)$ (ref. 8)

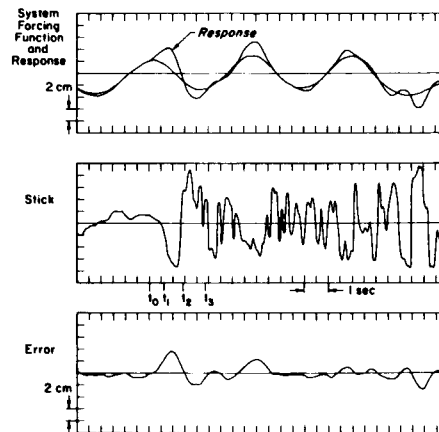


Figure 9. Transition from $4/s$ to $+8/s(s - 0.4)$ (ref. 8)

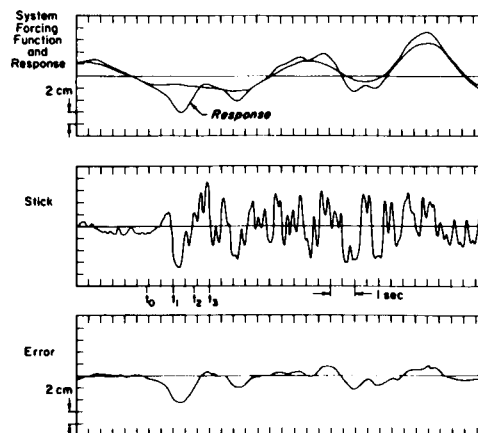


Figure 10. Transition from $4/s$ to $-8/s(s - 0.8)$ (ref. 8)

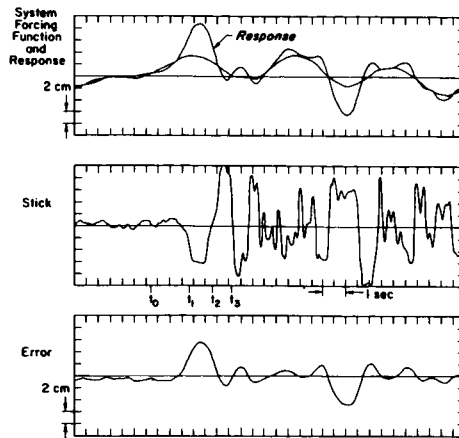


Figure 11. Transition from $4/s$ to $+8/s(s - 1.0)$ (ref. 8)

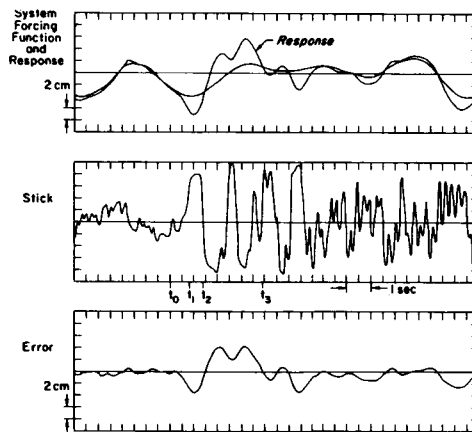


Figure 12. Transition from $4/s$ to $+8/s(s - 1.3)$ (ref. 8)

Transition Duration

The error traces of the transition data (particularly those of figs. 3 through 7) indicate that operator adaptation* occurs within about 3 sec in all cases. These fairly rapid transition times are representative of the average behavior observed in extensive experimental studies (refs. 4, 5, and 7) by Elkind, et al, of detection and adaptation times involving a variety of controlled elements and conditions. They are also compatible with Sadoff's results for his fixed-cab series (ref. 3).

It is obvious that the operator must adapt quickly to the new dynamics (or lose control) in the cases where the transition destabilizes the system (i.e., increase in order, large gain increase, etc.). In stable transitions where the system is not destabilized, there is no theoretical necessity for a rapid adaptation, however. That stable transition adaptations are rapid as well is an experimental fact demonstrated in reference 4 for pure gain transitions and in reference 11 for transitions with K/s controlled elements. These references show that adaptation is accomplished in 2 to 3 sec, even when the operator is not consciously aware that a transition has occurred.

While there appears to be a large amount of data showing rapid adaptation times, these results are by no means universal. Rapid adaptation times were generally not observed by Sadoff (ref. 3) in his moving-cab cases with the center-stick manipulator. In the data shown for the side stick under moving-cab conditions, however, the mean square error increases only a small amount following transition and remains constant for about 20 to 30 sec. This suggests that the adaptation may have been rapid, and the significant features of the data correspond to a post-transition adjustment phase. These longer apparent transition times might be attributable to differences between the center-stick and side-stick

*Adaptation time is roughly the time at which the transition response is completed, the operator has assumed the approximate form of the post-transition steady-state describing function, and has started reducing residual error to the asymptotic value.

manipulators. This does not appear too likely, however, since reference 12 shows that the operator adjusts his neuromuscular system characteristics to account for manipulator differences and exhibits roughly the same describing function over a broad range of devices.

Sadoff's fixed-cab conditions are generally compatible with the data shown in figures 3 through 7. Specifically, in three out of the five cases for fixed-cab center-stick control shown in reference 3, adaptation was accomplished in 3 to 6 sec. Thus, reasonably good correlation between data for similar experimental conditions appears to obtain.

The transition times observed by Sheridan (ref. 1) were not rapid either; however the controlled element variations occurred slowly with respect to typical adaptation times for step transitions. It may be concluded that he observed a posttransition adjustment phase characteristic rather than the step transition phenomena studied herein.

III. OPERATOR RESPONSE MODEL

The objective of this study is to obtain a model of the operator's dynamic response from the time of transition until the system error returns to within an acceptable threshold following operator adaptation to the new dynamics. Several types of transition models were considered at the outset of the study. These ranged from those which vary continuously with time in the manner of a learning servo, to ones which consist of a switched sequence of distinct modes having fixed characteristics. Of these, the mode-switching models are the only ones supported by the data. For example, a succession of distinct modes is strongly suggested by the sequence of distinct levels in the error response data of reference 3. As a result of these considerations, mode-switching models are the only ones considered in this report.

This section of the report examines the data of Section II, ultimately deriving a mode-switching model by induction. Observations of the data and analytical interpretations are commingled to some extent in order to best accomplish the model derivation.

Temporal Phases of a Transition Model

The available data suggest that there may be several temporal phases in the operator's response to a controlled element transition. Under this hypothesis, the several phases of a mode-switching model are defined and examined below with frequent reference to the data of Section II.

Pretransition retention. Initially, the operator acts as if the controlled element dynamics have not changed, and his adapted form, Y_{p1} , remains that pertinent to Y_{c1} . An incorrect stick deflection, $c(t)$, results; and the error increases according to $Y_{p1}Y_{c2}$ and the forcing function. The duration of this retention phase is governed by the time to exceed some error amplitude, and the operator's minimum latency in limiting cases. At the end of the retention phase the operator has detected that the controlled element has changed, but he does not know its form or gain.

The retention phase was first shown by Sadoff for both moving-cab and in-flight situations. Retention behavior following t_0 and prior to the first corrective response is clearly evident in the stick deflection traces of figures 3 through 7. In figure 3 stick deflection rate is approximately constant after t_0 and before the first little upward movement on the trace. Similarly, in the K_{C2}/s data (fig. 4) the retention is apparent during the 0.5 sec following t_0 and before the sharp upward movement on the stick deflection trace. The higher order transitions, figures 5 through 7, all involve a sign reversal in the controlled element which leads to a well defined stick reversal at the end of the retention phase, and the retention duration is readily recognizable in the data.

Transitions to the unstable controlled elements (figs. 8-12) all show well defined retention phases. The end of the retention phase is characterized by a sudden, rapid corrective stick movement that occurs at time t_1 shown on the data. This movement is particularly apparent in figures 10 and 12.

Optimal control. The operator's tasks following transition detection are to arrest the rate of divergence and reduce the error to some tolerable threshold level. The best way to accomplish this is to switch to an optimal mode of control following transition detection. For minimum transition time, a time-optimal or bang-bang model is hypothesized for this phase. Note that if only one set of data is found which evidences time-optimal response, that is sufficient to validate the model, at least as a useful limiting case. A considerable part of the experimental evidence in Section II supports a time-optimal response model as an appropriate idealization.

The available data for $Y_{C2} = K_{C2}/s^2$ presented in figures 5 and 7 suggest that a well trained operator responds in a way that is approximately time-optimal. The figure 5 data show a reversal at t_1 followed by a relatively long duration deflection or bang between t_1 and t_2 . This corresponds to the trajectory between points t_1 and t_2 for fixed bang amplitude on the illustrative phase plane of figure 13. The forcing function contributes a low frequency bias over the transition duration

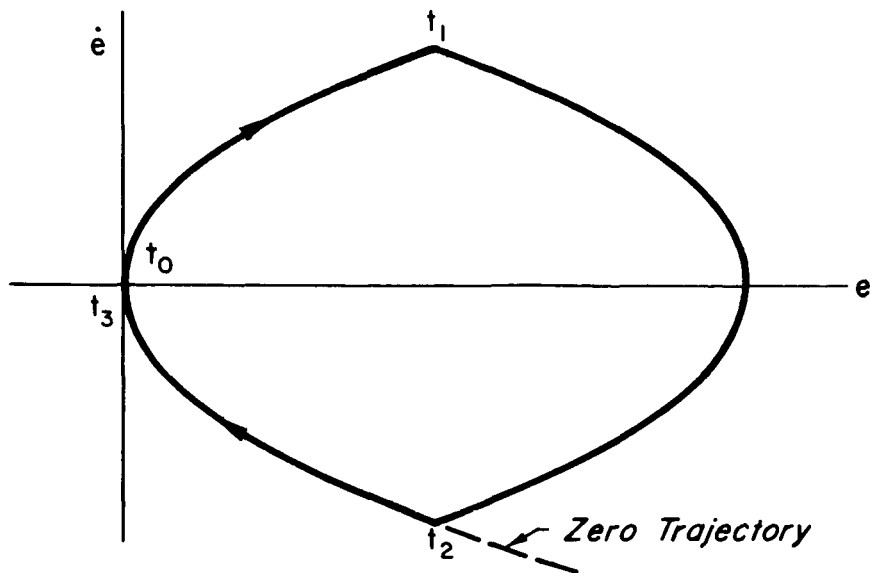


Figure 13. Phase plane trajectory for time-optimal control of K_{c2}/s^2

which can be neglected in the phase plane to a first approximation. At time t_2 another reversal occurs, and the system follows the zero trajectory into the phase plane origin, arriving at time t_3 , corresponding to the bang between times t_2 and t_3 in figure 5. At time t_3 the error and error rate are within the threshold region, the operator's deflection goes to zero, and he effectively "shuts off" this phase of the transition response. Thus, the figure 5 data exhibit nearly time-optimal response as evidenced by:

- The fixed bang amplitudes
- The minimum number of reversals
- Only one error peak with essentially no overshoot

The data in figures 6 and 7 show one extra reversal and an additional bang of short duration. This may result from an error in operator switching time, t_2 , caused by the forcing function. It could correspond to chatter in a suboptimal control mode near the error threshold region.

In figures 3 and 4 the polarity of the controlled element does not change, and the time-optimal response following retention would be to make a steplike increase in the magnitude of the stick deflection, $c(t)$,

to the bang amplitude. The stick would not be reversed. This is not evident in these data; instead, the operator reverses the stick incorrectly in each case, followed shortly by a second corrective reversal. The cause of these "reversal errors" appears to be that these nonpolarity reversal Y_c transitions were mixed in an experimental sequence with the others (figs. 5-7). Perhaps the operator adopts this reversal strategy ad hoc because the penalty in terms of loss of control for failing to reverse in the reversal cases is sufficiently greater than that incurred by a reversal error. This is particularly evident in the samples of figures 3 through 7 where all Y_c polarity reversal cases were of high order and difficult to control, while the nonreversal cases were of lower order and the error response to $c(t)$ was prompt, easily recognized, and readily controlled. In the ideal case the operator shouldn't make the reversal error, and it will not be included as an essential feature of the model. The possibility ought to be considered in an application nevertheless, particularly when the odds, penalties, or training favor the likelihood of a sign reversal at the time of Y_c transition.

The data of figures 8 through 12 correspond to controlled element transitions of the form

$$\frac{K_{c1}}{s} \rightarrow \frac{K_{c2}}{s(s - \alpha)}$$

The posttransition controlled element involves an integration plus a divergent inverse time constant, $-\alpha$, and its gain may be of either sign. The normalized phase plane for time-optimal control of this transition is given in figure 14 for the polarity reversal case. The retention period is from time t_0 to t_1 . The stick movement to start the optimal control phase occurs at time t_1 . A reversal to the second bang of the optimal control phase is required at time t_2 . The state then moves along the zero trajectory to the origin, the transition response is shut off at time t_3 , and the adjustment to posttransition steady-state tracking is made.

System control between times t_1 and t_3 is given by the block diagram of figure 15. The nonlinear computer reverses control at the zero trajectory. It is seen that the trajectories in figure 14 are not symmetrical

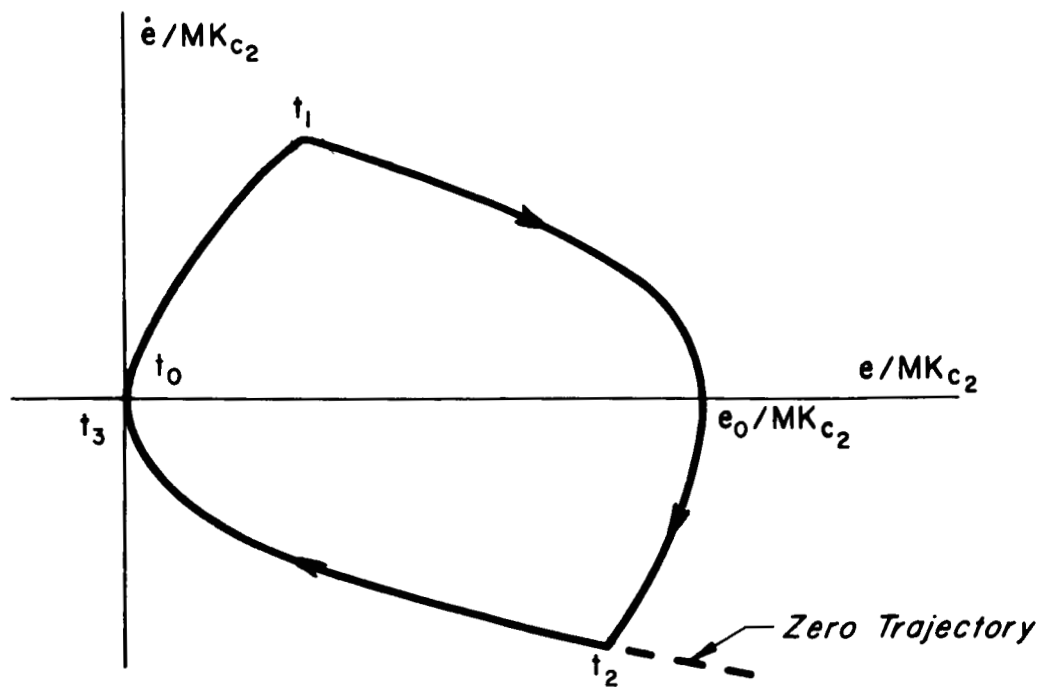


Figure 14. Phase plane trajectory for time-optimal control of $K_{c2}/s(s - \alpha)$

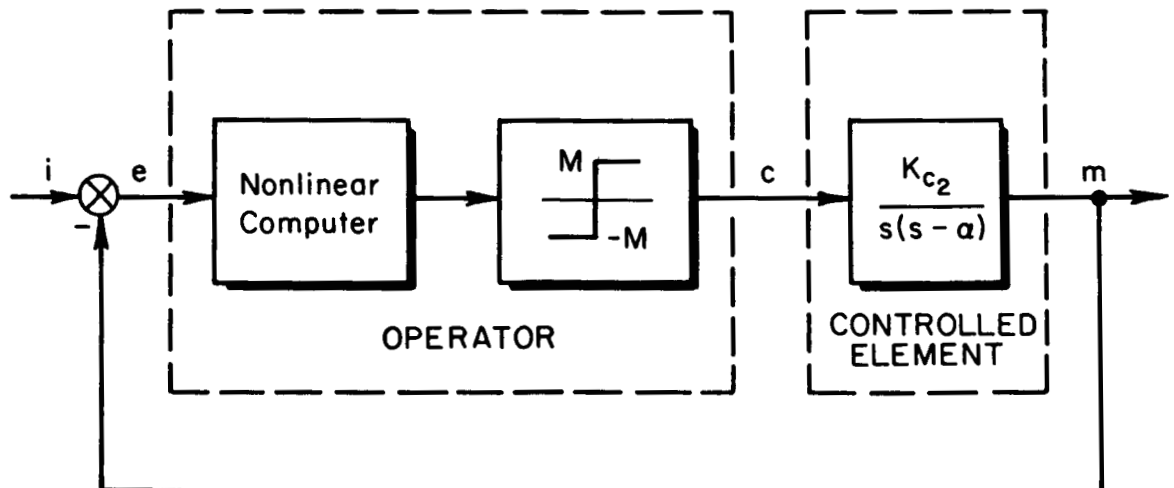


Figure 15. Time-optimal control for unstable controlled element

about the e/MK_{c2} axis because of the negative damping term. The trajectory from t_1 to t_2 through the point e_0/MK_{c2} is given (in the polarity reversal case) by

$$-\frac{\dot{e}}{MK_{c2}} + \ln \left(1 + \frac{\dot{e}}{MK_{c2}} \right) = -\frac{\alpha(e - e_0)}{MK_{c2}}$$

During the initial part of the trajectory after t_1 , the negative damping is opposing the applied torque and the system divergence is halted rather slowly for a given stick deflection, M . Once the error rate changes sign, its magnitude builds up rapidly because the applied torque is now aided by the negative damping. Following the reversal at time t_2 , the error converges rather slowly to the origin according to the equation

$$-\frac{\dot{e}}{MK_{c2}} + \ln \left(1 + \frac{\dot{e}}{MK_{c2}} \right) = -\frac{\alpha e}{MK_{c2}}$$

The shutoff time, t_3 , is highly critical, and a slight delay results in a rapid divergence and consequent error overshoot.

Idealized stick deflections and consequent error traces corresponding to the model response of figure 14 are sketched in figure 16. Several

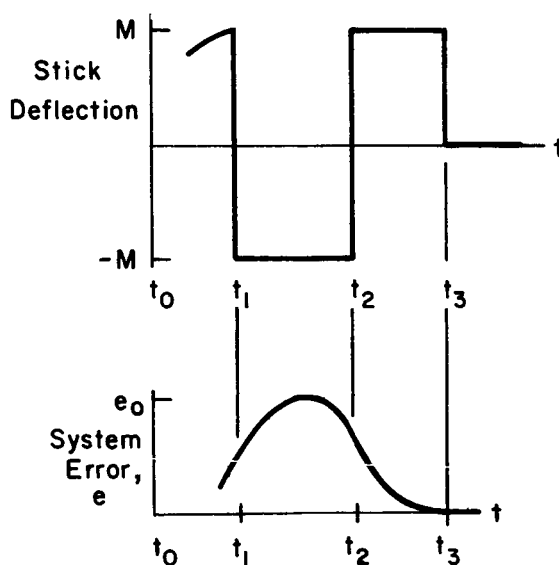


Figure 16. Ideal response for $K_{c1}/s \rightarrow K_{c2}/s(s-\alpha)$ transition

qualitative features that should be evident in any optimal response data for this type of transition are noted from figures 14 and 16:

- The retention phase should be relatively short when Y_c changes sign, due to the rapid buildup of e and \dot{e}
- The duration ($t_2 - t_1$) of the first bang should be relatively long in the case where Y_c changes sign, and short when it does not
- The stick reversal (at t_2) should occur shortly after \dot{e} changes sign

The data of figures 8 through 11 (summarized in Table II) show essentially optimal response for this phase. The nature of the error trace is a good clue to the degree of optimality. In the near-optimal cases there is only one dominant error peak with little overshoot. In figures 8, 9, and 11 the reversals are well defined. In figure 10 the second reversal is composed of pulselike steps. That the aggregate effect is near-optimal despite the pulsing is borne out by the data error trace. The effect of the pulsing on the phase plane trajectory can be shown as follows. Consider the idealized pulsing stick deflections of figure 17a having the corresponding phase plane trajectory sketched in figure 17b. It appears that the pulses are just "cautious steps" by the operator, and are good approximations to the single optimal reversal of the model at time t_3 .

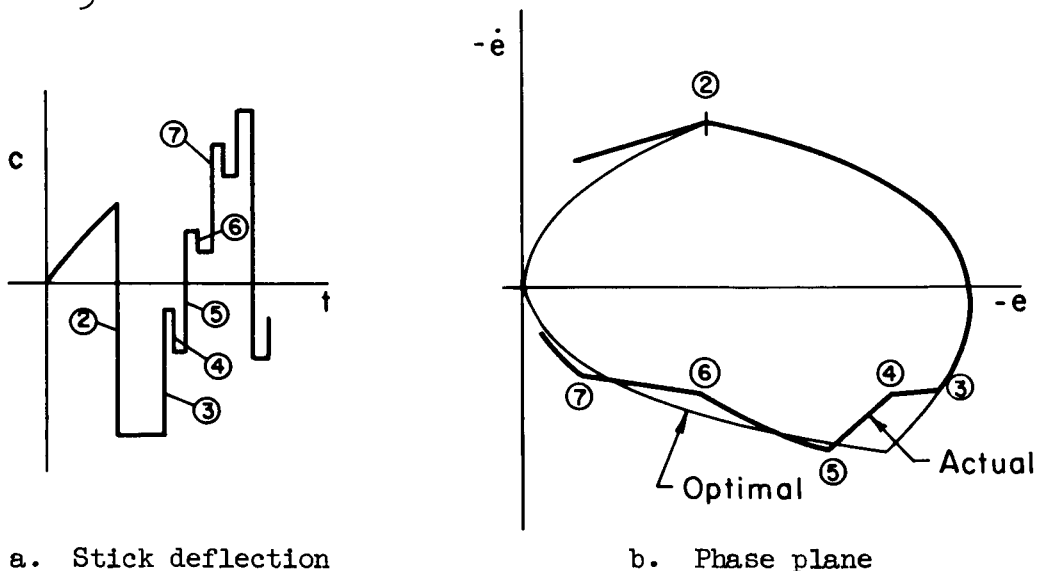


Figure 17. Effect of pulselike control

TABLE II
DATA DESCRIPTION

Fig. no.	Transition	Stick deflection record	Error record
8	$+ \frac{4}{s} \rightarrow \frac{-8}{s(s - 0.2)}$	Initial bang at t_1 builds up gradually. Second reversal is well defined. Bang amplitudes are approximately two-thirds stick limit.	Near optimal response, as evidenced by lack of error overshoot at time t_3 .
9	$+ \frac{4}{s} \rightarrow \frac{+8}{s(s - 0.4)}$	First bang and reversal at t_2 are well defined. Bang amplitudes are approximately two-thirds stick limit.	Delay of reversal at t_2 results in small error overshoot prior to shutoff.
10	$+ \frac{4}{s} \rightarrow \frac{-8}{s(s - 0.8)}$	First reversal well defined. Second reversal at t_2 composed of pulselike steps; see discussion and figure. Bang amplitudes are approximately two-thirds stick limit.	Near-optimal response, as evidenced by lack of error overshoot at time t_3 .
11	$+ \frac{4}{s} \rightarrow \frac{+8}{s(s - 1.0)}$	Reversals and bangs are well defined. Bang amplitudes are approximately two-thirds to three-fourths stick limit.	Delay of reversal at t_2 results in small error overshoot prior to shutoff.
12	$+ \frac{4}{s} \rightarrow \frac{+8}{s(s - 1.3)}$	Reversals and bangs are well defined. Bang amplitudes are about three-fourths stick limit. Extra stick reversals are required due to overshoot.	Delay of reversal at t_2 results in error overshoot. Greater instability of system results in increasing task difficulty.

Figure 12 shows nonoptimal response, presumably due to the large value of α , 1.3. A reasonable upper limit of α is about 1.5 for assurance of successful control, as shown in reference 13. This is for a skilled operator over a 4 min. period in a nontransition stationary tracking task in the presence of the same forcing function used herein. By comparison, in the stationary case with $\alpha=2$ the operator frequently loses control after only 20 to 30 sec of tracking (ref. 14).

The operator appears to be near-optimal more frequently in the transitions to the unstable second-order controlled element than for the simpler controlled elements, K_{c2} , K_{c2}/s , and K_{c2}/s^2 . This may be due to any or all of the following factors:

- **Task difficulty.** Task is more demanding than with the simpler controlled elements, and the operator must be a better controller to retain control.
- **Training.** Operator was more practiced and experienced, since these transitions were run toward the end of the experimental program after the simpler transitions (ref. 8).
- **Certainty.** The base case for these transitions was always K_{c1}/s , and transition to the unstable second-order Y_{c2} with some nominal α was a certainty. This could simplify the detection and identification process.

Evidence from nontransition control tasks exists to suggest that the operator has a time-optimal capability which can be utilized. In a series of experiments reported by Smith (ref. 15) the operator was told to track a "friction plus mass" controlled element "as fast as possible, or with the minimum of time delay." In 25 percent of these cases the operator response was that of a nonlinear time-optimal controller. Platzer's data (ref. 16) which used a phase plane display in a compensatory task show that the operator can respond time-optimally when given adequate switching information. The experiments of Pew (ref. 17) which employed a relay manipulator in control of K/s^2 forced the operator into a bang-bang mode and resulted in a stable limit cycle in the threshold region near the origin. More recent results obtained by Young and Meiry (ref. 18) using a third-order controlled element showed evidence of nonlinear bang-bang control by the operator.

Identification of Y_{c2} is important in determining the appropriate time-optimal control law to use during this phase. One method by which the operator may identify the controlled element is to use the basic property of the change in error due to his step change (or reversal) in $c(t)$ following retention. These properties are summarized in Table III for various orders of Y_{c2} . Notice that the identification is only a function of the posttransition controlled element under this hypothesis. A detailed investigation of detection and identification is reported by Miller in reference 9.

TABLE III
EFFECT OF STICK REVERSAL ON ERROR SIGNAL

Controlled element, Y_{c2}	Change in error signal due to step stick reversal
K_{c2}	Step change in error, $e(t)$
K_{c2}/s	Step change in error rate, $\dot{e}(t)$
K_{c2}/s^2	Step change in error acceleration, $\ddot{e}(t)$

Posttransition steady state. At the end of the time-optimal control phase, the error and its derivatives are reduced to within some threshold level. The operator then makes a mode switch to the steady-state quasi-linear describing function form appropriate to the new controlled element. That the operator eventually assumes a steady-state adaptation to the new controlled element is evident in all the data. The error and stick deflection traces in the data of Section II indicate that this adaptation happens rather quickly, particularly in the more difficult transitions. Also, by mode-switching from bang-bang time-optimal control to quasi-linear control when the error and error rate are reduced to within some threshold, the problem of limit cycling near the origin which would occur in the nonlinear model is avoided. This adjustment to the posttransition steady state with its quasi-linear control is the last phase of the mode-switching model.

The Resultant Transition Model

The data of Section II appear to confirm the time-optimal control mode-switching model to the extent that it is a good simplification of and mean estimator for operator transition response behavior. The three successive control modes used to explain operator response actions following a step change in controlled element among the general forms K , K/s , and K/s^2 are summarized in Table IV. Operator behavior in the entire period between pretransition and posttransition steady-state tracking is defined in terms of either duration, solution to an optimal control problem, or Y_{p1} and Y_{p2} .

Prediction of transition behavior would proceed in the stepwise manner outlined in Table IV. The retention phase has a duration based on data for various controlled elements. The next phase might involve a phase plane analysis with the selected form of controller. When system error and error rate are reduced to within some threshold level, a mode-switch to the quasi-linear describing function for posttransition steady-state control is made. The optimal response phase for the unstable second-order controlled element was examined in figures 14 through 16 in connection with the data interpretation. Similar analyses for K/s and K/s^2 post-transition controlled elements are given below.

In the K_{c2}/s case, the optimal control phase of the model takes the simple form of figure 18. No nonlinear computer is required in the operator block—only the relay. The normalized phase plane trajectories for

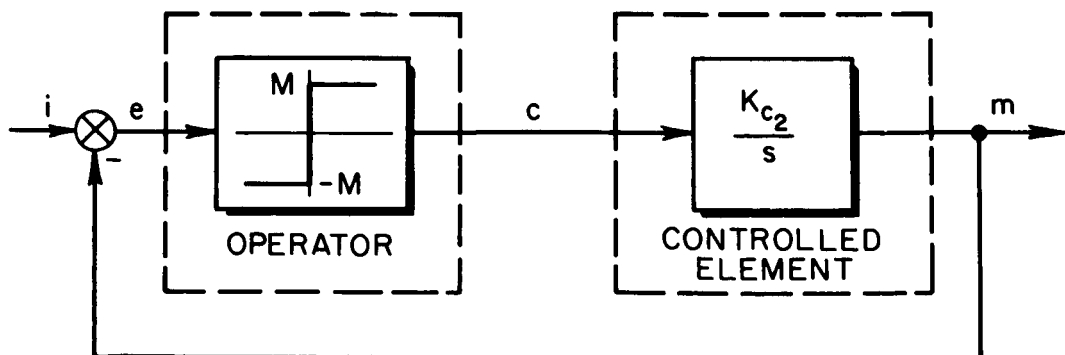


Figure 18. Time-optimal control for first-order system

TABLE IV
MODE-SWITCHING TRANSITION MODEL SUMMARY

Response phase	Mode-switching model	Duration and timing		Description
0 Pretransition steady state	<p style="text-align: center;">$-\infty < t < t_0$</p>			Quasi-linear compensatory tracking
1 Pretransition retention	<p style="text-align: center;">$t_0 \leq t \leq t_1$</p>	Posttransition controlled element	Approximate duration (sec)	Transition occurs at $t = t_0$. The operator continues tracking with the pretransition adaptation. An incorrect still deflection and error buildup occur as functions of $i(t)$ and Y_{c2} . At time t_1 , the operator has detected the transition and ceased retention behavior.
2 Optimal control	<p style="text-align: center;">$t_1 < t < t_3$</p>	K_{c2} K_{c2}/s K_{c2}/s^2	0.2 0.5 1.0	Just after t_1 , the operator adopts either an optimal or suboptimal mode of control. The simplest hypothesis is the use of a nonlinear optimal controller. Variation of parameters such as control amplitude, M, provides one suboptimal form. Quasi-linear control with lead and time delay provides another.
Posttransition steady state	<p style="text-align: center;">$t \geq t_3$</p>			Quasi-linear compensatory tracking

constant stick deflection, M , are as shown in figure 19. Following transition the error and error rate move into the first or third quadrant of figure 19, depending on $Y_{p1} Y_{c2}$ (and, in practice, the forcing function). As the divergence moves to point t_1 on the phase plane, the operator reverses the stick due to the error buildup. The system moves instantaneously along the line $t_1 - t_1$ in figure 19 at the time of reversal because Y_{c2} is first-order. Only one bang is required during the optimal control phase, and the trajectory goes directly into the threshold region. At point t_3 the control mode switches to quasi-linear control appropriate to the posttransition steady state, and the deflection returns to zero. Note that any positive deflection, M , following the reversal is acceptable, and the key control problem is the shutoff time.

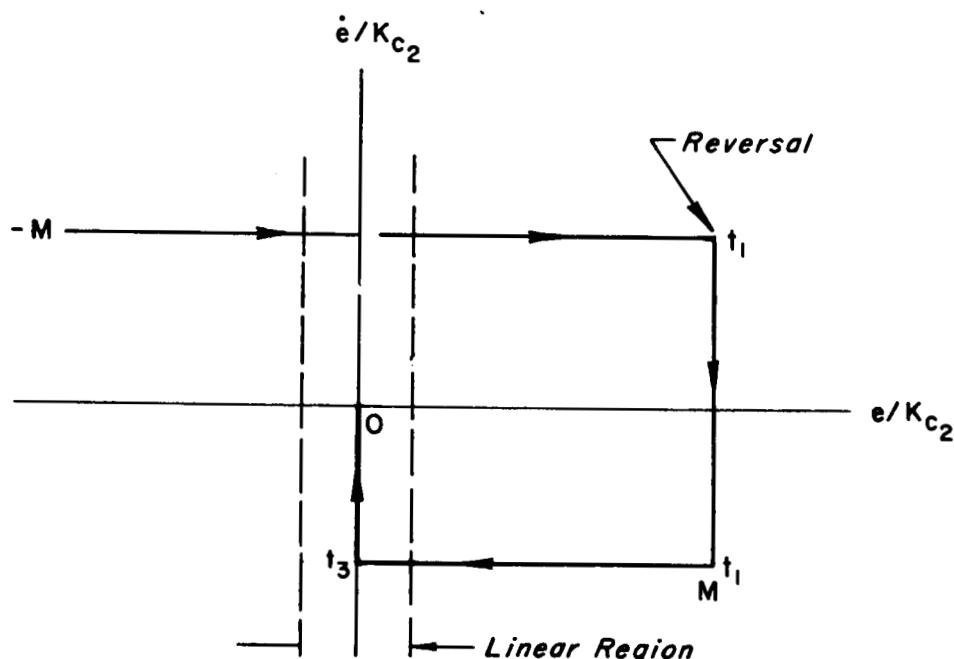


Figure 19. Phase plane trajectories for first-order system

The effect of forcing function can be quite significant in the first-order case. It may result in incorrect behavior in the optimal control phase, because it can make the system state (e and \dot{e}) appear to be divergent in the first quadrant of figure 19 (for example) when it is actually convergent in the fourth quadrant. This results in an incorrect reversal of the stick.

For the second-order controlled element transition, K_{c2}/s^2 , the optimal control phase block diagram takes the form of figure 20. The nonlinear

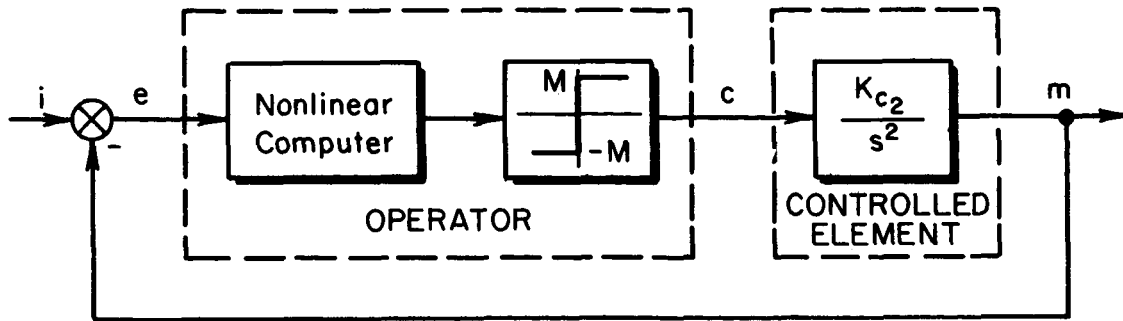


Figure 20. Time-optimal control for second-order system

computer reverses the control at the zero trajectory or switching line. The switching lines for the $Y_{c2} = K_{c2}/s^2$ case and zero forcing function are given by

$$\dot{e} = -\sqrt{2MK_{c2}}|e| \operatorname{sgn} e$$

The normalized phase plane portrait and switching lines for this second-order system are given by the parabolic trajectories in figure 21.

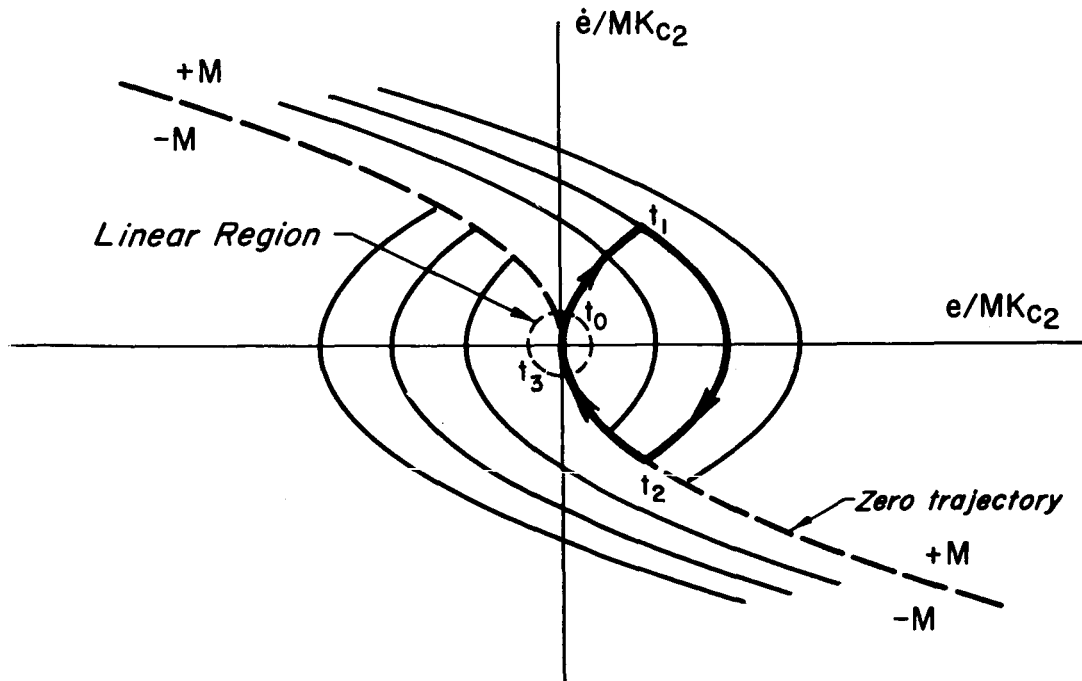


Figure 21. Phase plane trajectories for simple second-order system

During the retention phase immediately following the transition to K_{c2}/s^2 , the operator attempts to reduce the error with his pretransition adaptation. The error and error rate increase into either the first or third quadrant of the phase plane, depending on $Y_{p1}Y_{c2}$ and (to a small extent) the forcing function. The reversal at t_1 on the phase plane of figure 21 leads to the first bang of the optimal control phase. It results in a trajectory which is stable until the switching line or zero trajectory is reached. The next step is to reduce the error and error rate to zero in an optimal way. This requires a second reversal at t_2 when the zero trajectory is reached. The model mode-switches to quasi-linear control at t_3 when the error and error rate are reduced to within a threshold region near the origin. In some data (e.g., fig. 7) the operator appears to overshoot the zero trajectory. This may put him in the region of the origin, but requires an additional reversal and a short duration bang to remain within the error threshold. In figure 5, on the other hand, his response appears to be near optimum with negligible overshoot.

The derived model has the distinct advantage for predictive purposes that one can apply time-optimal control theory to manual control problems. It appears to be a reasonably close approximation to all the limited data available and is the only model which will provide an accurate description of those data which are indeed time-optimal. Suboptimal interpretations and models for the optimal control phase are possible alternatives, but to validate their use requires (1) demonstration that the operator response is not time-optimal, and (2) sufficient experimental evidence to permit a choice between competing suboptimal forms.

Limitations of the Transition Model

The duration of the retention phase is not given by a set of logical rules in the model. It depends on the operator transition detection criterion. Retention durations for a variety of controlled elements and differential controlled elements are known experimentally, however, and typical results are shown in Table IV.

The amplitude of the bangs is not given by the model. Some maximum deflection will be used with a free-moving manipulator, while a maximum force level will be used with an isometric device.

The effect of forcing function may be important. The model is derived from response data for a low frequency random input. Higher frequency inputs could modify the results; however, they are unlikely to be encountered in a closed-loop vehicle analysis. The forcing function may lead to analytical difficulties in the optimal control phase in predictive applications of the model. Inclusion of the input effect in a phase plane analysis is laborious and inexact, and analog or digital computation may simplify this aspect of response prediction.

As proposed, the model will explain or predict operator response during transitions among controlled elements of the forms K , K/s , K/s^2 , and $K/s(s - \alpha)$. Additional data are required to sustain its more general applicability to other controlled elements.

Experimental results obtained by Sadoff (ref. 3) in a moving-cab simulator with a center-stick manipulator do not agree with extant fixed-base data, or with moving-cab data with a side stick. Consequently, derived models based on these data are apparently not applicable to controlled element transitions in moving cabs with center stick. This may limit the applicability of the derived model to the in-flight transition problems which are of prime interest.

IV. CONCLUSIONS AND RECOMMENDATIONS

A mode-switching model of the human operator during controlled element transitions has been derived on the basis of extant data. Three successive control modes are used to explain operator response following transitions among the forms K , K/s , K/s^2 , and $K/s(s - \alpha)$. Operator behavior in the entire period between pretransition and posttransition steady-state tracking is defined in terms of either duration, solution to an optimal control problem, or Y_{p1} and Y_{p2} .

Conclusions

Operator response and adaptation to step changes in the controlled element occur quickly, and in most cases are completed within a few seconds. This is true even for transitions involving only a small reduction in the controlled element gain, which are not consciously detected by the operator until long after his adaptation is completed. The only known exceptions are the results obtained in the moving-cab with center-stick manipulator.

The mode-switching models are the most appropriate with which to characterize operator transition response. Models which vary continuously with time, for example learning servos, do not appear to be valid. This is particularly evident in the light of Sadoff's error data which show that the control technique changes do occur suddenly.

There are sufficient data which demonstrate nearly time-optimal control characteristics to say that this form of control is a valid intermediate phase in the transition model. Conversely, it is the only form of model which will explain those response data which are indeed time-optimal.

The model describes the transition data in the simplest way, and in a minimum number of steps. It ties in directly with the known pretransition and posttransition steady-state characteristics of the operator.

Recommendations

Additional experimental work is needed to validate the proposed transition model, and the nature of transition response should be measured in detail for a more complete set of transition situations. In addition, the effect of the following experimental variables should be examined:

Forcing function. The effect of forcing function bandwidth should be determined, from both the standpoint of operator response and the effect on analytic predictions with the model.

Task order. The effect of sequence of transition and number of alternatives should be studied more fully, as well as the effect of the difference between the pretransition and posttransition controlled elements. A rational basis for the prediction of reversal errors should be established.

Motion cues. The effect of motion cues on transition response should be examined in more detail, in order to determine why the experimental results in the moving-cab case differ from those for the larger body of fixed-base data.

Display. The results of reference 16 suggest that the use of a phase plane display (\dot{e} versus e) by a trained operator yields a substantial improvement in performance over the one-dimensional compensatory display. A similar improvement may occur during transitions.

Training. The data show both optimal and suboptimal behavior modes during transition, suggesting that any one of several alternative controller forms might result from the learning process. Perhaps an operator who evidences suboptimal response can be instructed in the best way to obtain more optimal transition response and hence better performance.

REFERENCES

1. Sheridan, Thomas B.: Time-Variable Dynamics of Human Operator Systems. Tech. Rep. [Contract AF 19(604)-4548; AFCRC-TN-60-169, ASTIA AD-237045], Eng. Proj. Lab., Dept. of Mech. Eng., Mass. Inst. of Tech., Mar. 1960.
2. Sheridan, Thomas B.: Studies of Adaptive Characteristics of the Human Controller. Tech. Rep. DSR-8055-5 (ESD-TDR-62-351), Eng. Proj. Lab., Dept. of Mech. Eng., Mass. Inst. of Tech., Dec. 1962.
3. Sadoff, Melvin: A Study of a Pilot's Ability to Control During Simulated Stability Augmentation System Failures. NASA TN D-1552, 1962.
4. Young, Laurence R.; Green, David M.; Elkind, Jerome I.; and Kelly, Jennifer A.: The Adaptive Dynamic Response Characteristics of the Human Operator in Simple Manual Control. NASA TN D-2255, 1964.
5. Elkind, J. I.; Kelly, J. A.; and Payne, R. A.: Adaptive Control Characteristics of the Human Operator in Systems Having Complex Dynamics. IEEE Proceedings of the Fifth National Symposium on Human Factors in Electronics, May 1964.
6. Elkind, J. I.: Human Operator Response to Changing Controlled Element Dynamics. Bolt, Beranek, and Newman, Inc., May 1963.
7. Kelly, J. A.; and Elkind, J. I.: Adaptation of the Human Operator to Changes in Control Dynamics. Rep. MR-10124-1, Bolt, Beranek, and Newman, Inc., 15 Mar. 1964.
8. Elkind, Jerome I.; and Miller, Duncan C.: Adaptive Characteristics of the Human Controller of Dynamic Systems. Bolt, Beranek, and Newman, Inc. (AFFDL-TR-66-60), July 1966.
9. Miller, Duncan Charles: A Model for the Adaptive Response of the Human Controller to Sudden Changes in Controlled Process Dynamics. B.S. and M.S. Thesis, Mass. Inst. of Tech., 1965.
10. Elkind, Jerome I.; and Miller, Duncan C.: On the Process of Adaptation by the Human Controller. Paper presented at Third Congress of the International Federation of Automatic Control, London, 20-25 June 1966.
11. McDonnell, J.: A Preliminary Study of Human Operator Behavior Following a Step Change in the Controlled Element. Tech. Memo. 133-2, Systems Technology, Inc., Feb. 1965.

12. Magdaleno, R. E.; and McRuer, D. T.: Effects of Manipulator Restraints on Human Operator Performance. Tech. Rep. 134-2 (forthcoming AFFDL Tech. Rep.), Systems Technology, Inc., Apr. 1966.
13. McRuer, Duane; Graham, Dunstan; Krendel, Ezra; and Reisener, William, Jr.: Human Pilot Dynamics in Compensatory Systems — Theory, Models, and Experiments with Controlled Element and Forcing Function Variations. Tech. Rep. 115-1 (AFFDL-TR-65-15), Systems Technology, Inc., Jan. 1965.
14. Jex, H. R.; McDonnell, J. D.; and Phatak, A. V.: A "Critical Task" for Man-Machine Research, Related to the Operator's Effective Delay time. Part I. Theory and Experiments with a First-Order Divergent Controlled Element. Tech. Rep. 147-1 (forthcoming NASA CR), Systems Technology, Inc., Aug. 1965.
15. Smith, Otto J. M.: Nonlinear Computations in the Human Controller. IRE Trans., vol. BME-9, no. 2, Apr. 1962, pp. 125-128.
16. Platzner, H. L.: Nonlinear Approach to Human Tracking. Interim Tech. Rep. I-2490-1, The Franklin Institute, 21 Dec. 1955.
17. Pew, R. W.: A Model of Human Controller Performance in a Relay Control System. IEEE Proceedings of the Fifth National Symposium on Human Factors in Electronics, May 1964.
18. Young, L. R.; and Meiry, J. L.: Bang-Bang Aspects of Manual Control in High-Order Systems. IEEE Trans., vol. AC-10, no. 3, July 1965, pp. 336-341.

00975
183 up
26-1-67

"The aeronautical and space activities of the United States shall be conducted so as to contribute . . . to the expansion of human knowledge of phenomena in the atmosphere and space. The Administration shall provide for the widest practicable and appropriate dissemination of information concerning its activities and the results thereof."

—NATIONAL AERONAUTICS AND SPACE ACT OF 1958

NASA SCIENTIFIC AND TECHNICAL PUBLICATIONS

TECHNICAL REPORTS: Scientific and technical information considered important, complete, and a lasting contribution to existing knowledge.

TECHNICAL NOTES: Information less broad in scope but nevertheless of importance as a contribution to existing knowledge.

TECHNICAL MEMORANDUMS: Information receiving limited distribution because of preliminary data, security classification, or other reasons.

CONTRACTOR REPORTS: Technical information generated in connection with a NASA contract or grant and released under NASA auspices.

TECHNICAL TRANSLATIONS: Information published in a foreign language considered to merit NASA distribution in English.

TECHNICAL REPRINTS: Information derived from NASA activities and initially published in the form of journal articles.

SPECIAL PUBLICATIONS: Information derived from or of value to NASA activities but not necessarily reporting the results of individual NASA-programmed scientific efforts. Publications include conference proceedings, monographs, data compilations, handbooks, sourcebooks, and special bibliographies.

Details on the availability of these publications may be obtained from:

SCIENTIFIC AND TECHNICAL INFORMATION DIVISION
NATIONAL AERONAUTICS AND SPACE ADMINISTRATION
Washington, D.C. 20546